

## **SUPPLEMENTAL FIGURE LEGENDS**

Figure S1 (related to Figure 2). Additional connecting cilia STORM reconstructions of markers for sub-ciliary regions. Reconstructions corresponding to (A, B) Fig. 2B, (C) Fig. 2C, (D). Fig. 2D. Select regions from connecting cilia (CC) STORM reconstructions are shown magnified below (red dotted boxes and arrow). (B) 50 nm thick profiles are demonstrated to establish the acTub profile compare to centrin-2. Images on each row of each panel share the same scale bars. Yellow arrows = CC STORM clusters extending to ciliary membrane. Orange arrows = STORM clusters in OS (identified in DIC images). Stars = basal body/inner segment localization.

Figure S2 (related to Figure 2). Additional connecting cilia STORM reconstructions of IFT81 and IFT88. Replicate reconstructions corresponding to (A) Fig. 1D, and (B) Fig. 1E. Select regions from connecting cilia (CC) STORM reconstructions are magnified (red dotted box and arrow). All CC reconstructions and magnifications are of the same scale, respectively, and share the same scale bars. Yellow arrows = CC STORM clusters of interest. Orange arrows = OS STORM clusters of interest. Stars = basal body/inner segment STORM clusters. Stars = basal body/inner segment STORM clusters.

Figure S3 (related to Figures 3-5). Additional STORM reconstructions showing localization of BBS5 (A, C), BBS9 (B, C) and STX3 (D). In panel C, the left-most image shows wide-field TUBA1 immunofluorescence to mark the CC (dashed line). Red arrows and boxes indicate regions of images enlarged below (A, D) or to the right (B,

C). All CC reconstructions and magnifications are of the same scale, respectively, and share the same scale bars. Stars = BB/IS STORM cluster. Orange arrows = OS localization.

Figure S4. (related to all Figures). Additional IFT88/BBS5 colocalization STORM reconstructions (A-C). (A) DIC and widefield fluorescence of a TUBA1 + IFT88 + BBS5 3-color immunostained mouse retina thin section. (B) STORM reconstruction from the same section as (A) then overlaid with the TUBA1 widefield image to mark CC boundaries. A single CC is isolated and magnified (red dotted arrow). The colocalization pattern of IFT88 and BBS5 is further magnified for clarity. (C) Replicate STORM reconstructions corresponding to Fig. 3. All CC reconstructions and magnifications are of the same scale, respectively, and share the same scale bars. Stars = basal body/inner segment localization. Yellow arrows = BBS5 localization surrounding IFT88 clusters. White arrows = An IFT88 cluster isolated from BBS5. Orange arrows = colocalization of IFT88 and BBS5 in the OS region. (D) DIC images of WT and three BBS mutant retinas (*Bbs2*<sup>-/-</sup>, *Bbs2*<sup>-/-</sup>, *Bbs2*<sup>-/-</sup>), showing partial preservation of OS at 8 weeks post-natal. (E) Confocal fluorescence images of mouse retina cryosections for all antibodies and labeling reagents used for immunostaining and STORM in this study.

Figure S5 (related to Figures 6 and 7). Effects of BBS deficiencies on BBS5 and syntaxin-3 localization. (A, B) Widefield immunofluorescence of BBS5 (A), centrin 2 (A), acTub (B) and STX3 (B) in WT and *Bbs* mutant mice. Ages for mutant mice: *Bbs2*<sup>+/-</sup> & *Bbs2*<sup>-/-</sup> = 8 weeks, *Bbs4*<sup>+/-</sup> = 8 weeks, *Bbs4*<sup>-/-</sup> = 5 weeks, *Bbs7*<sup>+/-</sup> and *Bbs7*<sup>-/-</sup> = 8 weeks.

A line is traced above the acTub positive connecting cilia (CC) to mark the boundary between outer segment (OS) and inner segment (IS). All images are of the same scale and share the same scale bar. White arrows = mislocalizations to the OS in knockout examples. (C, D) Quantitative analysis of perturbations in STX3 distribution. (C) Ripley's K-function of adjacent example STX3 STORM reconstruction clustering in WT and *Bbs* mutants reveals a more diffuse distribution within the CC in the mutants. (D) Graph of STX3 radial localization at the CC for WT and *Bbs* rods. Middle bars mark the mean values with error bars marking the standard deviations. The radius of STX3 STORM reconstructions does not differ significantly in *Bbs* vs WT CC, except for *Bbs7<sup>-/-</sup>* (Student's t-test. \*  $P < 0.05$ ).

Figure S6 (related to Figure 6). Additional STORM reconstructions for BBS5 and centrin-2 in *Bbs* mutant rod photoreceptors. All *Bbs* mutant retinas are from age 7-8 week mice, except for 5 week old examples of *Bbs4<sup>-/-</sup>*, (C). Rod outer segment ("Rod OS") STORM examples from a wider view are depicted to demonstrate OS mislocalization. Dashed lines show regions magnified in adjacent images. All CC reconstructions are the same scale. Stars = BB/IS STORM clusters. Orange arrows = aberrant BBS5 localization in the OS. Cyan arrows = normal BBS5 localization in the OS. White arrows = Centrin-2 mislocalization puncta in the OS.

Figure S7 (related to Figure 7). Additional STORM reconstructions for STX3 and acTub in *Bbs* mutant rod photoreceptors. (A) *Bbs2<sup>-/-</sup>*, (B, C) *Bbs4<sup>-/-</sup>*, (D) *Bbs7<sup>-/-</sup>*. Ages are as

indicated. Dashed lines show regions magnified in adjacent images. Stars = BB/IS  
STORM clusters. Orange arrows = STX3 mis-accumulation in the OS.

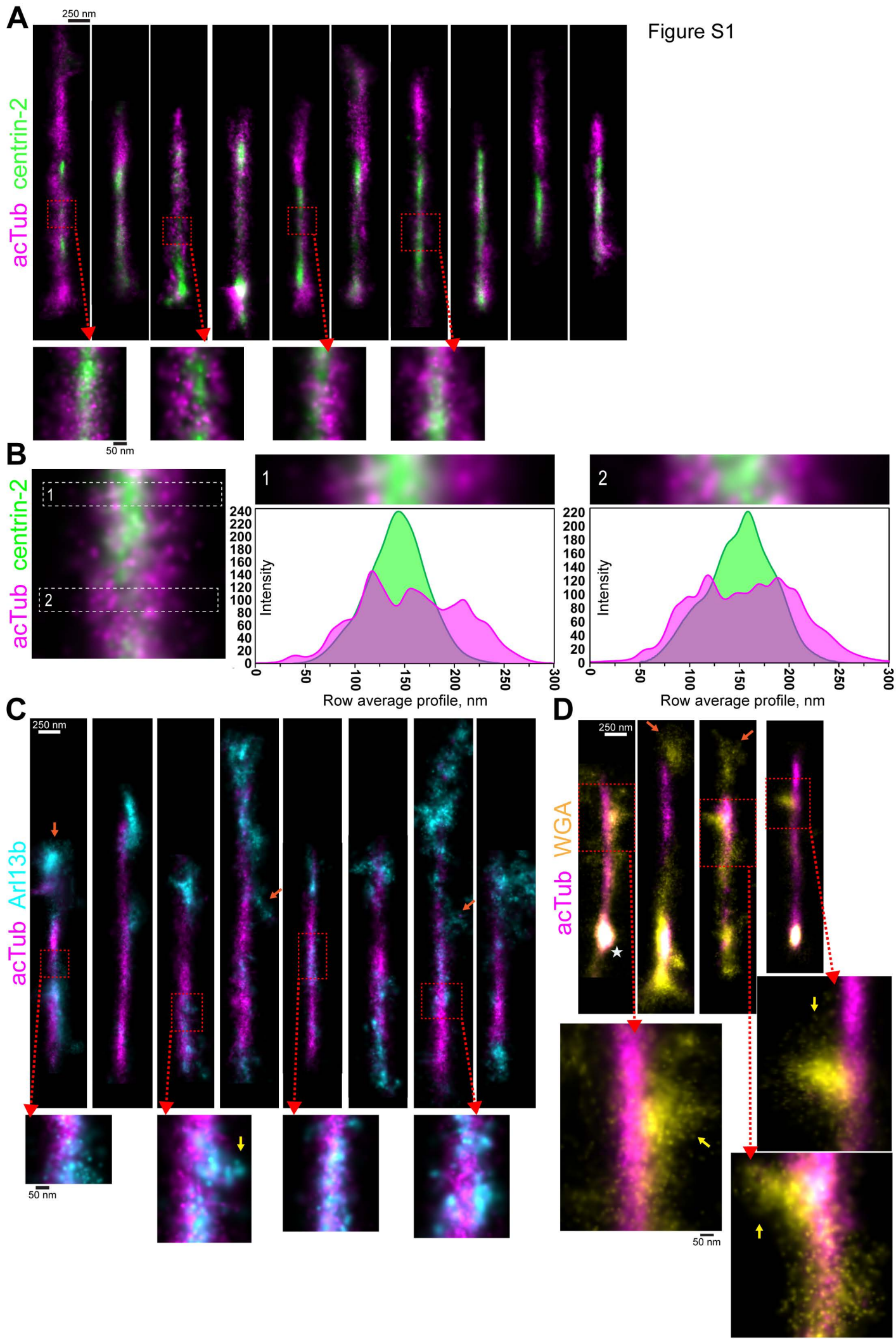
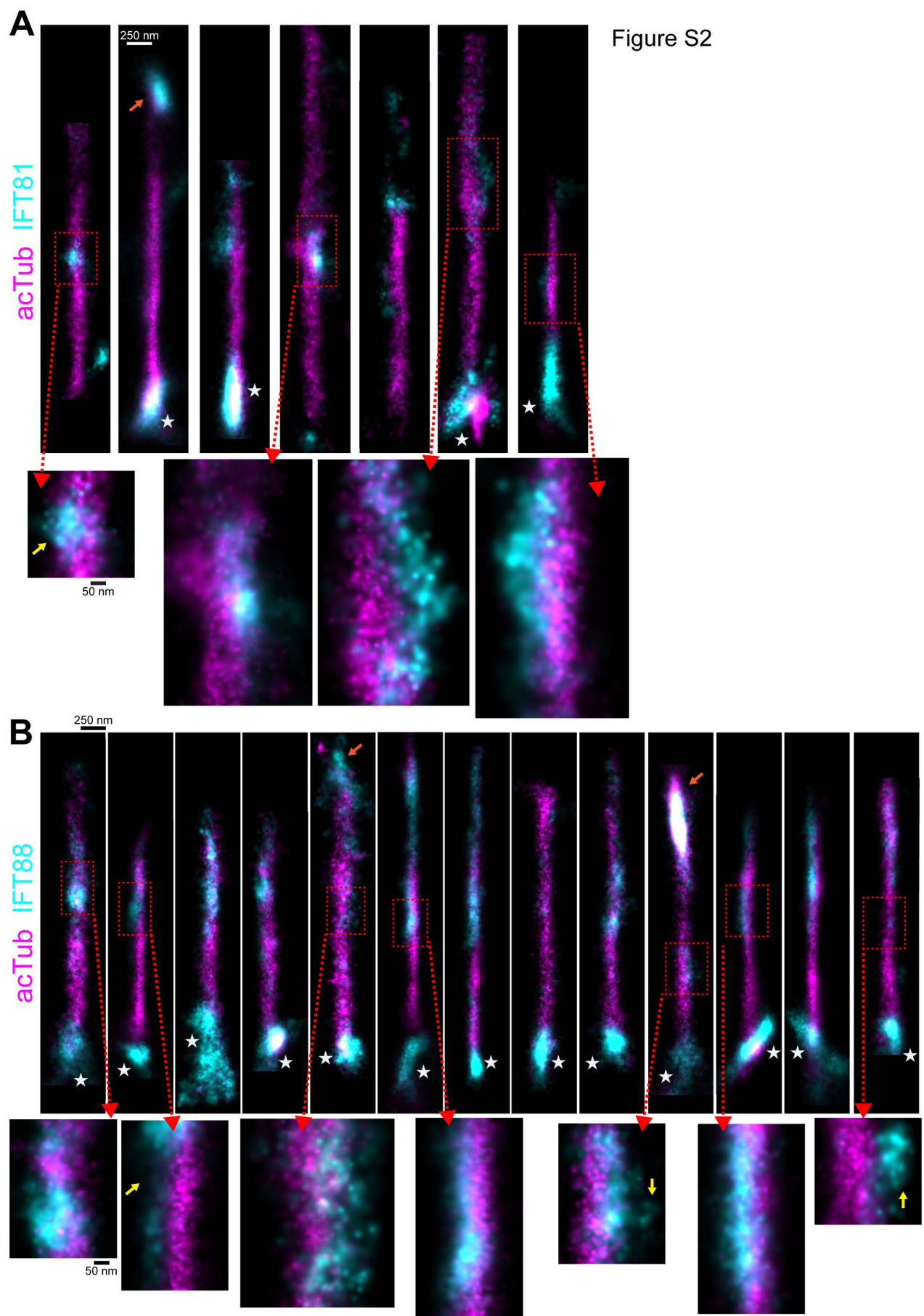


Figure S2



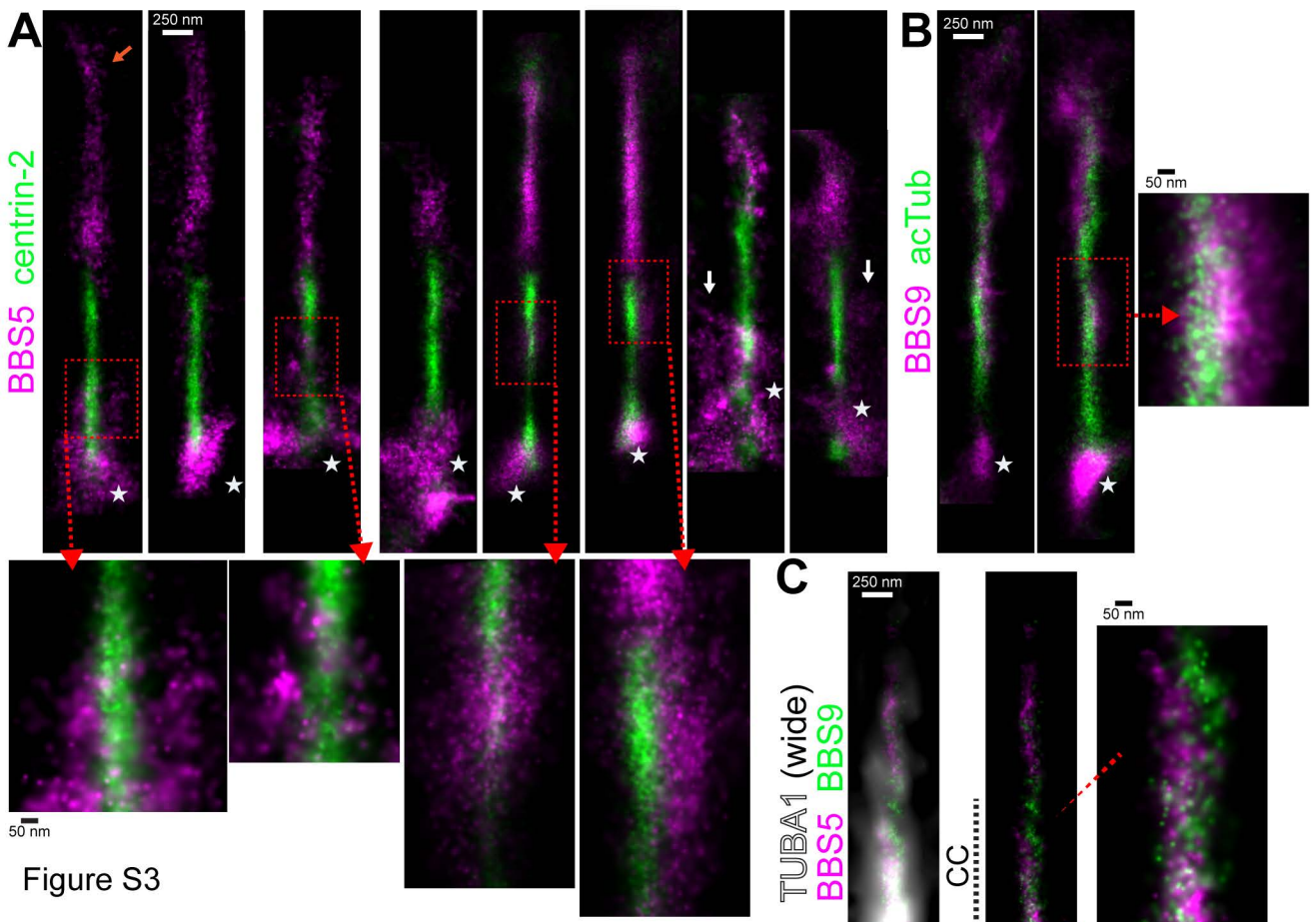
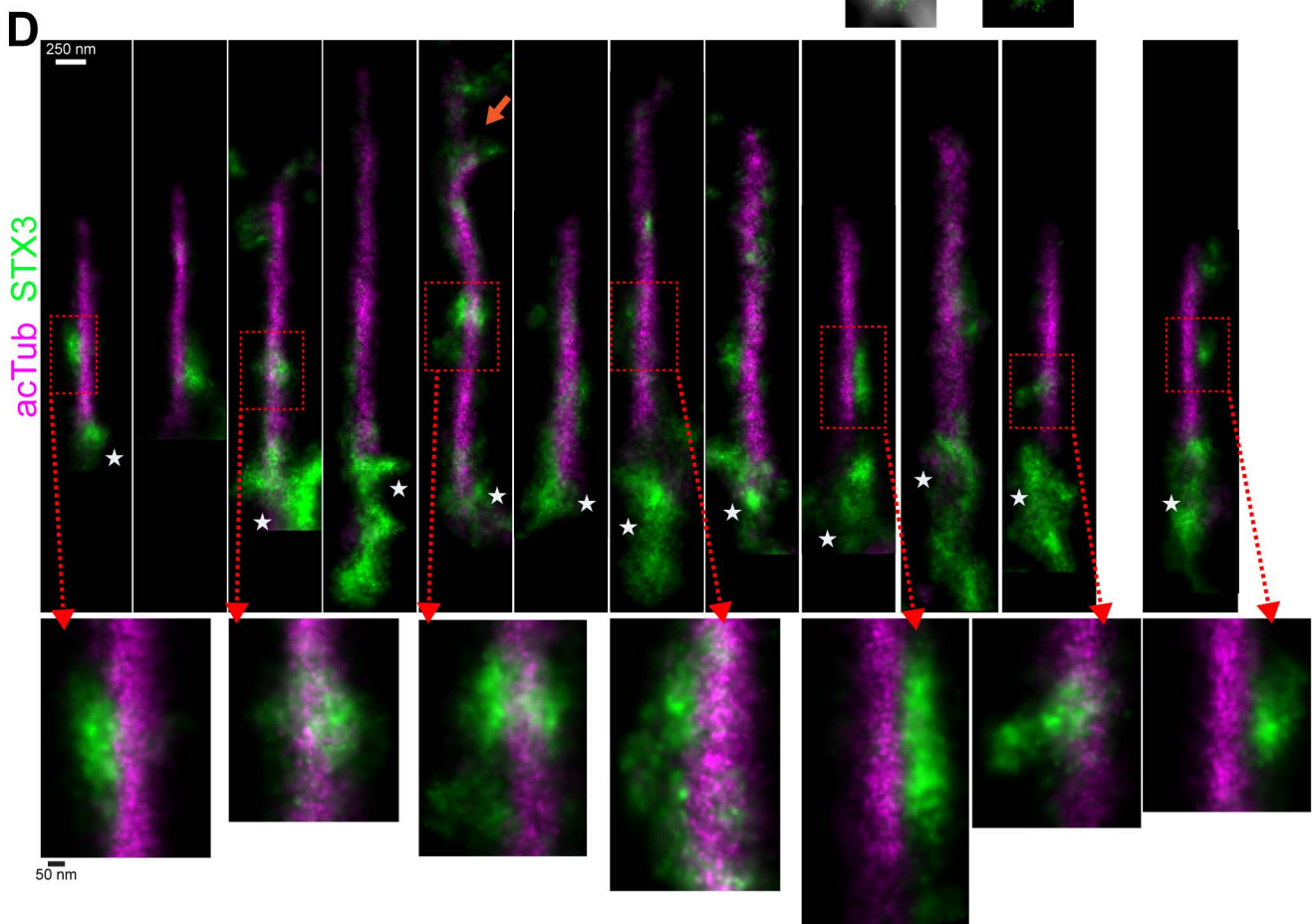
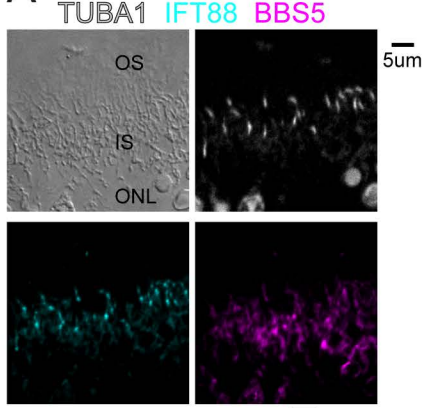


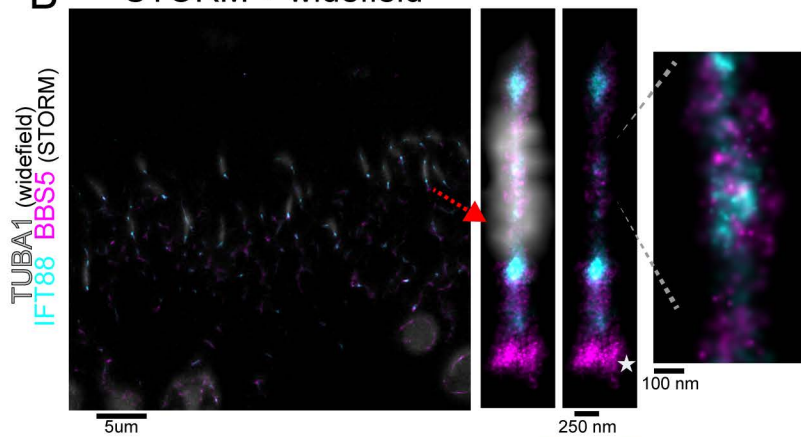
Figure S3



**A** Widefield  
TUBA1 IFT88 BBS5



**B** STORM + widefield



**C**

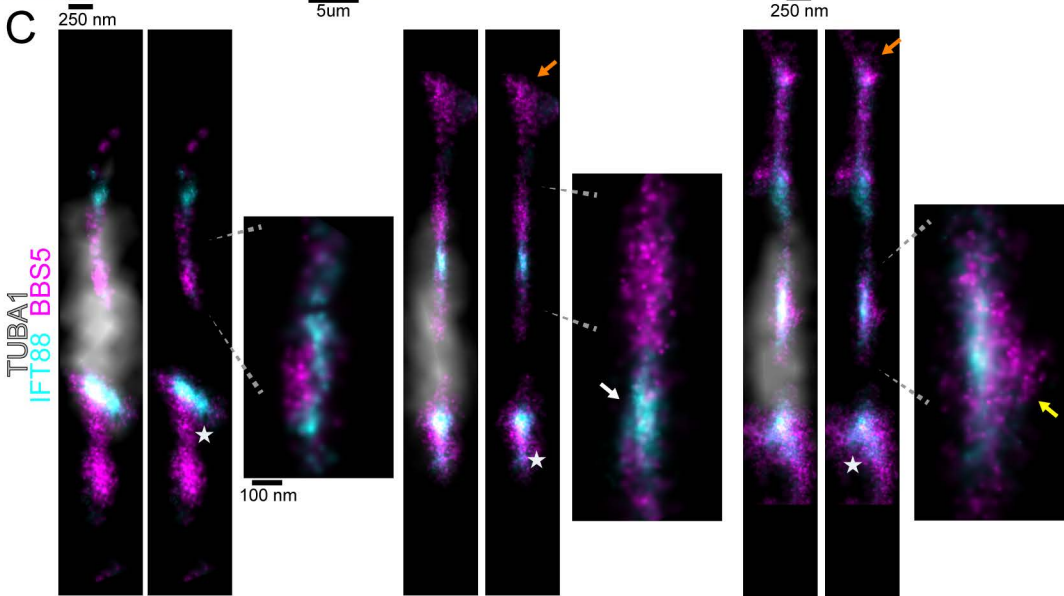
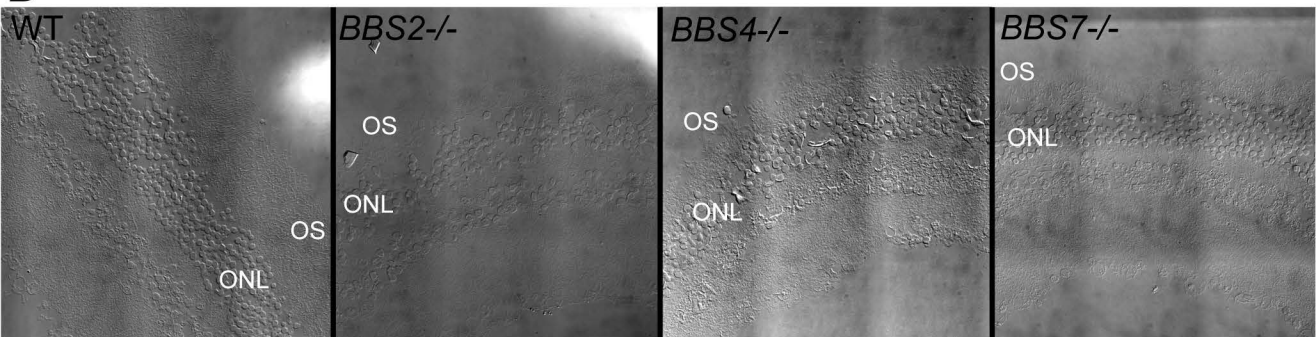
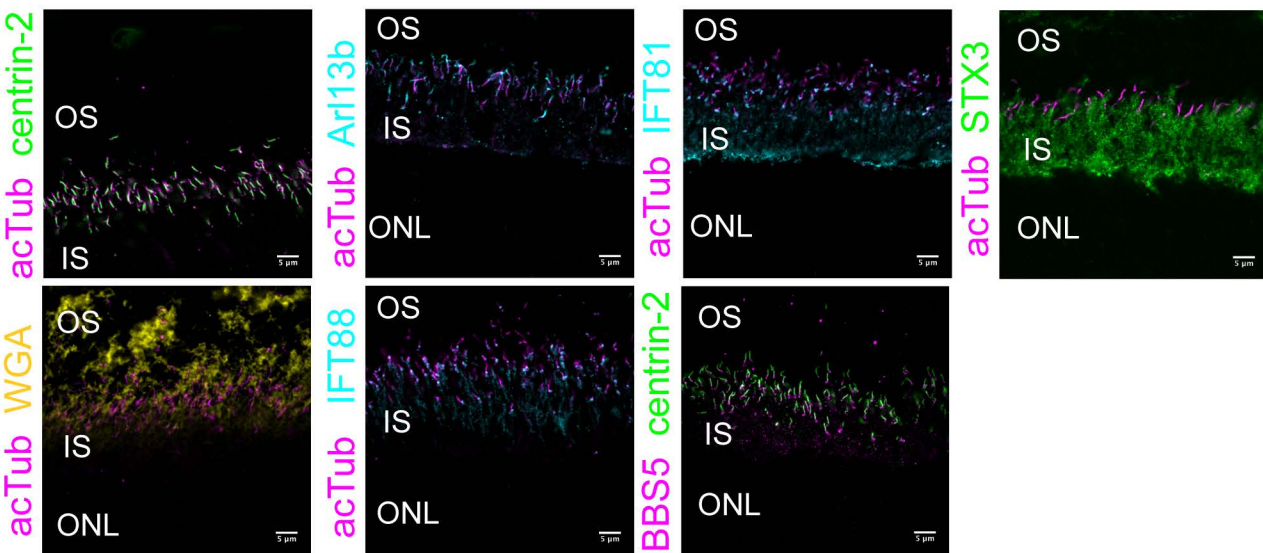


Figure S4

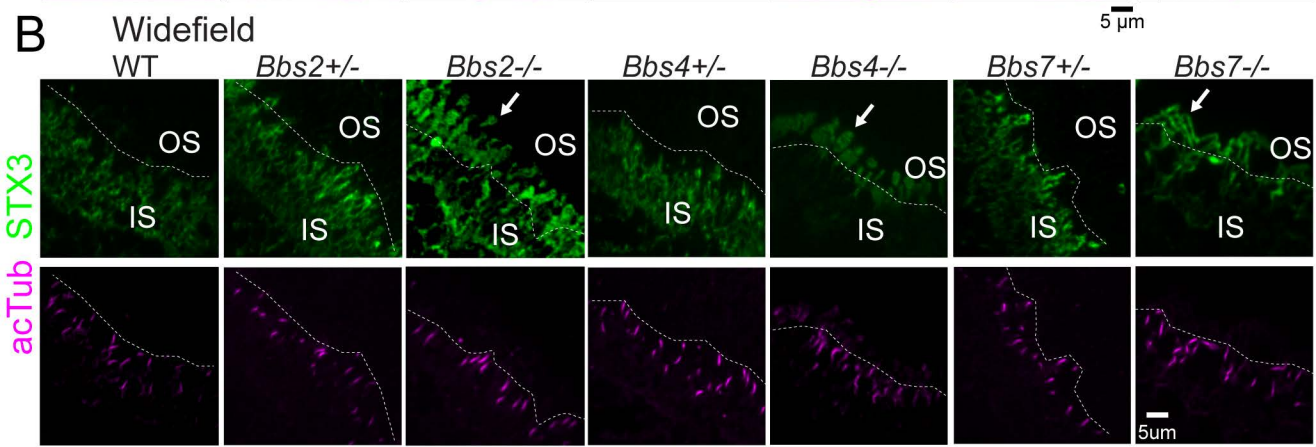
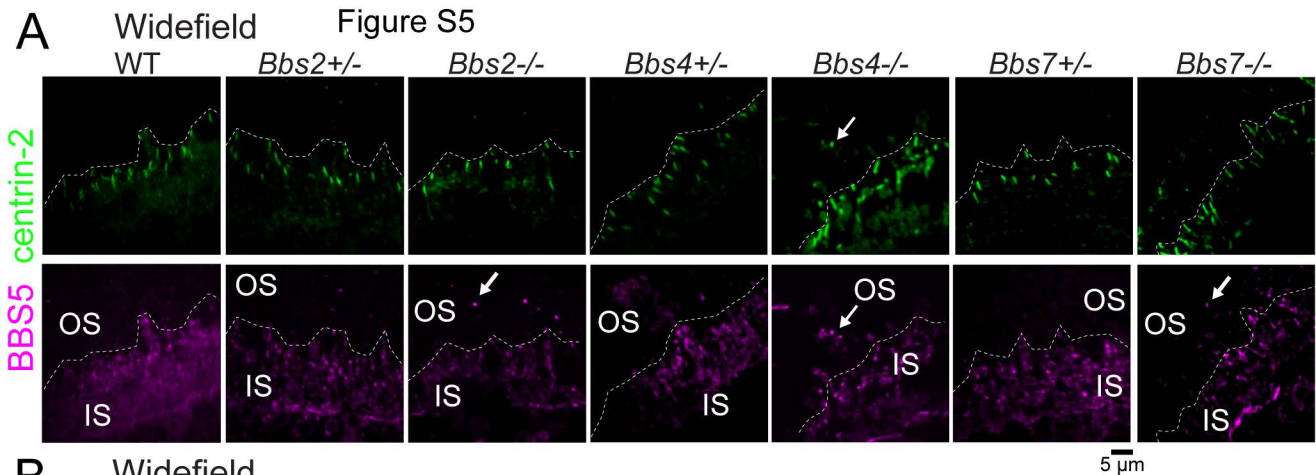
**D**



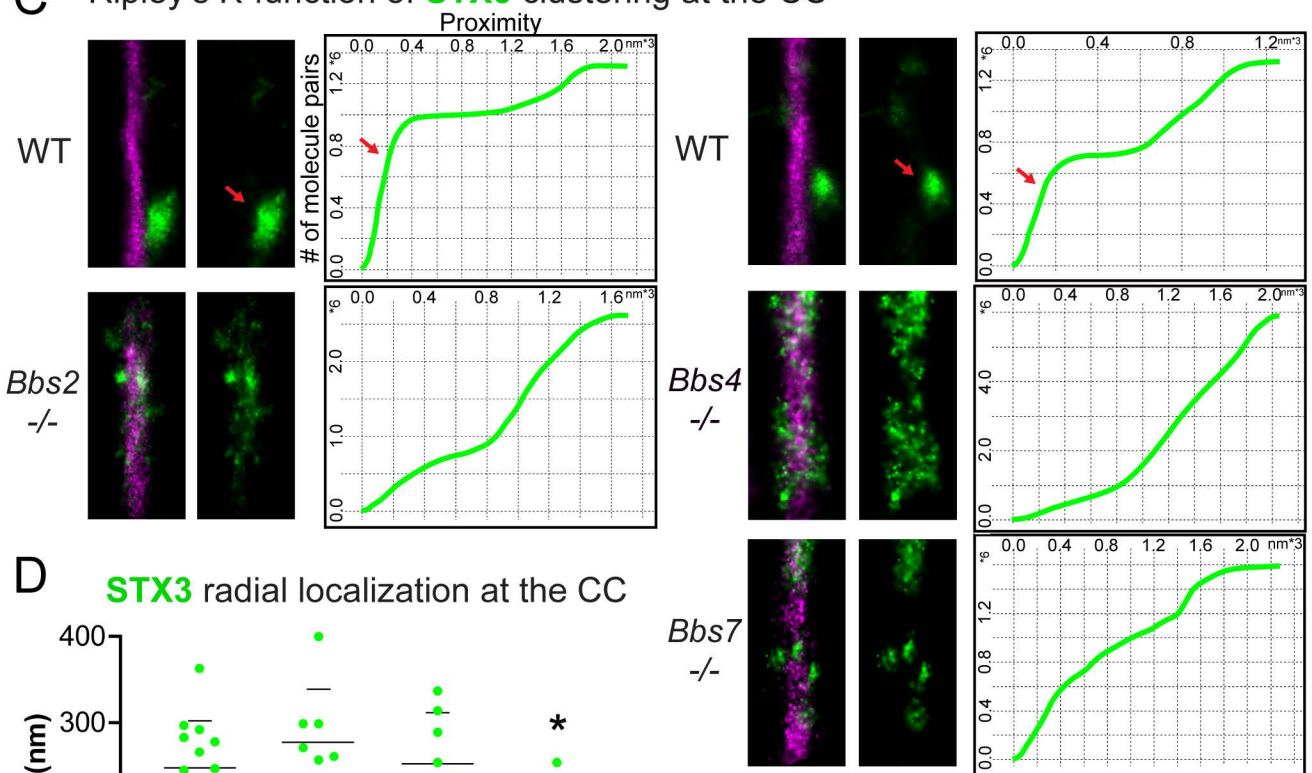
**E**







**C** Ripley's K-function of **STX3** clustering at the CC



**D** **STX3** radial localization at the CC

